Appendix II

Controlling the Binding Orientation of Tailless Hairpin Polyamides

Abstract

Most hairpin polyamides exhibit a binding orientation preference aligning N-terminal to C-terminal along the DNA in the 5' to 3' direction. It has been postulated that this orientation preference is caused by the C-terminal alkyl tail of the polyamide molecule. With recent advances in the solid-phase synthesis of polyamides, molecules without C-terminal tails are now accessible. We find that these tailless polyamides exhibit severely reduced orientation preference when compared to their tail-containing counterparts. We find that installation of (R)-diaminobutyric acid at the turn position is able to restore preference for "forward" binding. However, installation of the (S)-diaminobutyric acid does not favor "reverse" binding.

Introduction.

Pyrrole-imidazole hairpin polyamides bind the minor groove of DNA with high affinity and sequence specificity.[1] Most hairpin polyamides synthesized to date bind with the N-terminus oriented towards the 5' end of the DNA.[2] It has been postulated that the C-terminal alkyl tail is responsible for the orientation preference of minor groove-binding polyamides.[3] Indeed, the natural products distamycin and netropsin closely resemble polyamides in structure (Figure II.1). Structural studies have found that distamycin possesses a strong orientation preference when bound in 2:1 complexes with polyA-DNA, favoring

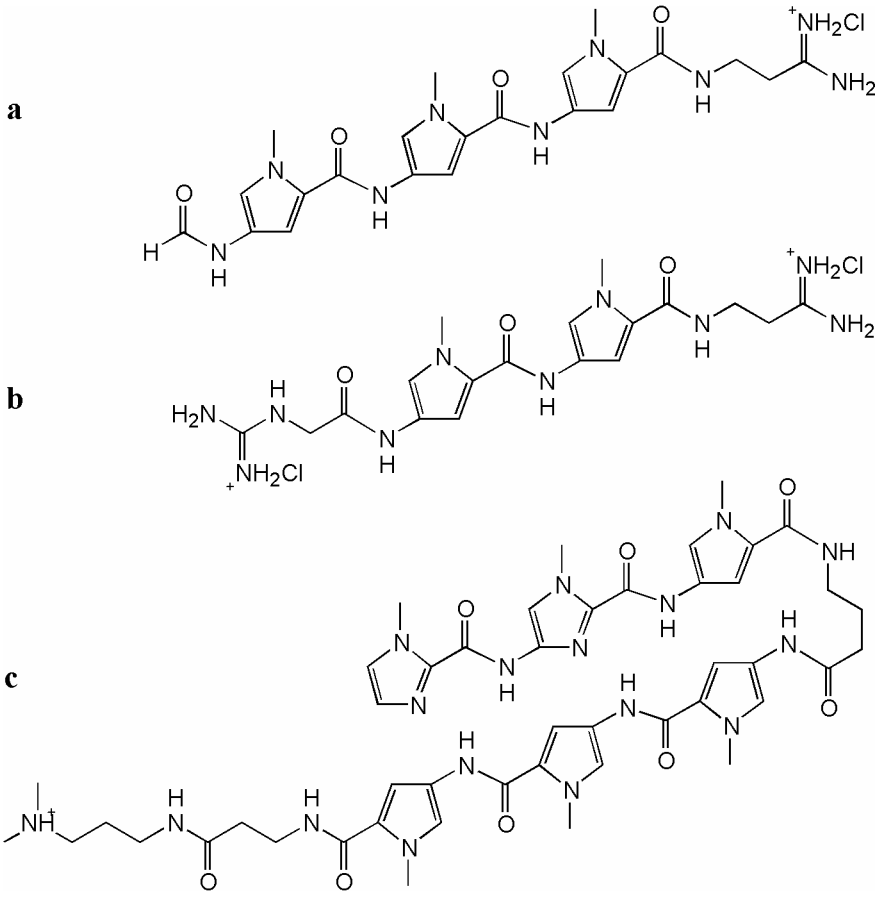

Figure II.1. Structures of minor groove-binding agents distamycin (a); netropsin (b); pyrrole-imidazole polyamide with β-Dp tail (c).

N-terminal alignment with the 5' end of the DNA by greater than 20:1.[4-6] Conversely, netropsin bound to the same sequence of DNA exhibits only a 3:2 orientation preference.[7] Indeed, the most obvious structural difference between these two molecules is that netropsin has an alkyl tail at both its C- and N-termini, while distamycin has only a C-terminal tail.

NMR structures of a 6-ring hairpin polyamide bound to the minor groove in both the "forward" (N→C aligning 5'→3') and "reverse" (N→C aligning 3'→5') orientations reveal interesting structural characteristics. All structures reveal a twist in the ligand that

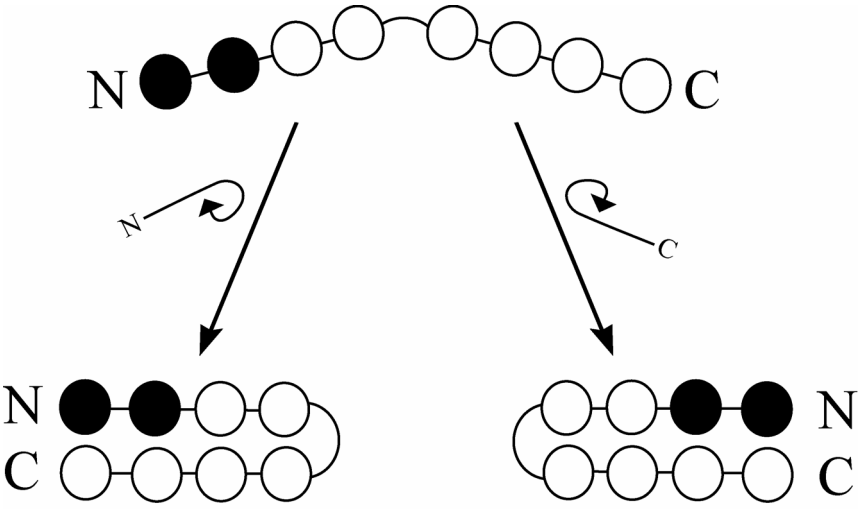

Figure II.2.[8] Model for the two folding geometries of a hairpin polyamide. Folding pathways lead to hairpin structures suitable for recognition of DNA in the forward orientation (left) and reverse orientation (right). Pyrrole and imidazole carboxamides are represented by white and black circles, respectively.

allows it to better match the curvature of the DNA. When bound in the forward orientation, the twist allows the C-terminal tail to lie along the floor of the groove. Conversely, when bound in the reverse orientation, the twist would cause the C-terminal tail to sterically clash with the wall of the minor groove, and as a result, the tail points out into solution in order to avoid this clash.[3] Thus, when bound in the reverse orientation,

polyamides lose the favorable hydrophobic interactions between the alkyl tail and the hydrophobic minor groove.

For any given hairpin polyamide core, there exist two, non-superimposable hairpin folds that are related by mirror plane symmetry (Figure II.2).[8] The binding of these two folds to DNA is energetically distinguished by the tail effects described above, thus leading to the experimentally observed orientation preference. With the recent advances in solid-phase synthesis methodology,[9] tailless polyamides are now synthetically accessible. Because the orientation preference of polyamides is postulated to be a direct consequence of the presence of the C-terminal tail, these tailless polyamides may not have any orientation preference.

Recent studies have shown that installation of a chiral amine on the γ-aminobutyric acid "turn" residue acts as an additional determinant for orientation preference. When polyamides are functionalized with the (R)-enantiomer of γ-aminobutyric acid they possess high affinity and specificity for forward orientation binding. When the (S)-enantiomer is installed, binding affinity at the forward orientation match site is reduced almost 200-fold (note, the compound still possesses a slight preference for the forward binding site due to the presence of a C-terminal β-Dp tail).[8] Computer-generated models show that the differences in binding are caused by differential placement of the amine functionality. In the forward orientation, the (S)-enantiomer causes the amine to sterically clash with the wall of the minor groove, while the (R)-enantiomer allows the amine to point freely out of the minor groove.[8]

In this study, we are interested in whether the enantiomers of the γ-aminobutyric acid turn can control the binding orientation of tailless hairpin polyamides. In the

absence of a C-terminal tail, the chiral turn should be the only determinant of binding orientation. As shown in figure II.3, the (R)-chiral turn should favor the forward orientation, but disfavor reverse orientation binding, while the (S)-chiral turn should favor reverse binding and disfavor the forward orientation.

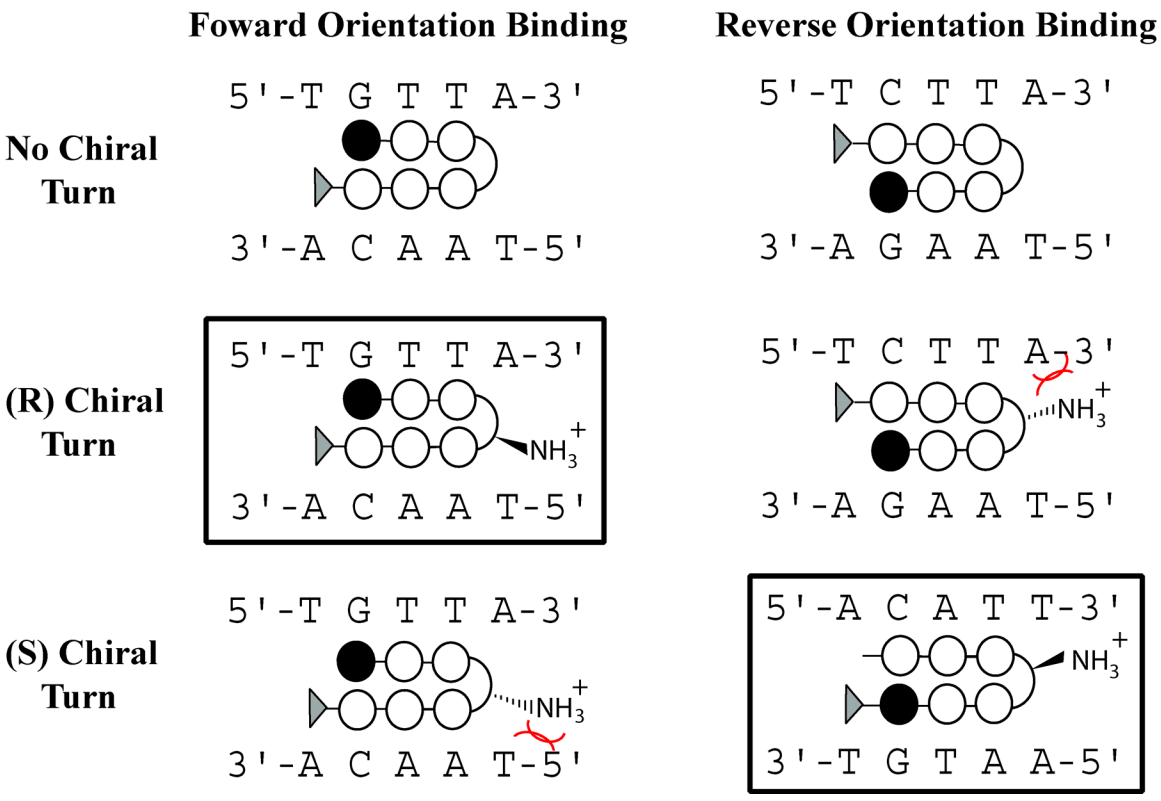

Figure II.3. Schematic representation of how the chiral turn may be used to control binding orientation of tailless hairpin polyamides. Top row, unfunctionalized tailless polyamides should not possess any orientation preference. Middle row, Functionalization with the (R)-chiral turn should favor the forward binding orientation (boxed) and lead to a steric clash with the wall of the minor groove when bound in the reverse orientation. Bottom row, Functionalization with the (S)-chiral turn should favor the reverse binding orientation (boxed) and lead to a steric clash with the wall of the minor groove when bound in the forward orientation.

Results.

Polyamides **ATK-iix-73**, **ATK-iix-74**, **ATK-iix-75**, **ATK-iix-76**, and **ATK-iix-77** were synthesized on oxime resin using standard reagents and procedures (Figure

II.4).[9] Each polyamide was designed to contain a single positive charge. Compounds **ATK-iix-74** and **ATK-iix-76** are analogs of **ATK-iix-73** and **ATK-iix-75**, respectively, in which the chiral amine has been acylated. The acyl group provides additional steric bulk in a stereocontrolled manner, and should accentuate any orienting effects of the chiral group. Compound **ATK-iix-77** is the control compound with no functionality at

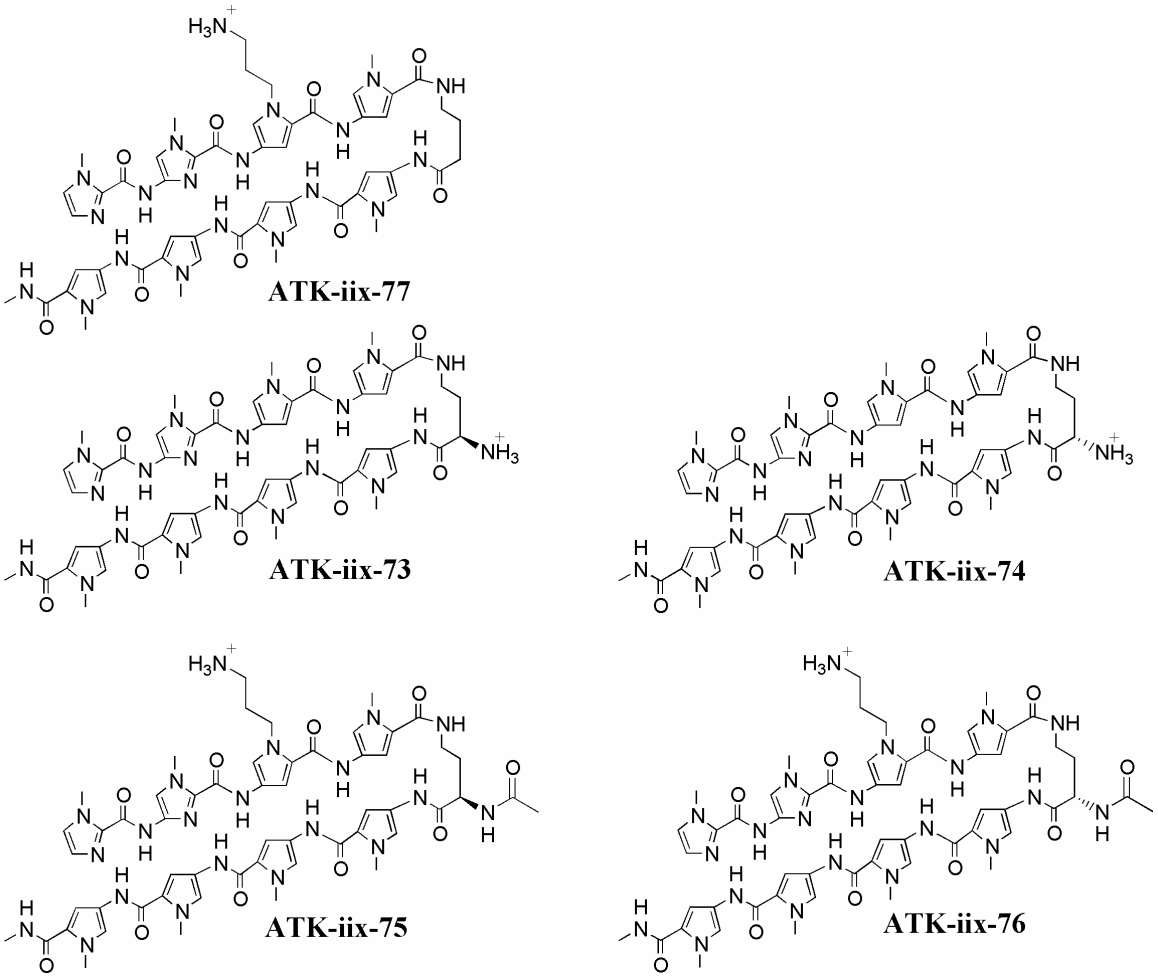

Figure II.4. Chemical structures of the hairpin polyamides synthesized for this study. Each polyamide is designed to recognize the sequence WGGWWW (where W = A or T). Each polyamide has a single positive charge.

the turn position. The β-Dp analog of **ATK-iix-77** has previously been footprinted, and binds with an association constant of 1.9 x 10^9 M^{-1} (at 5'-TGGTAT-3'), exhibiting >500-fold preference for forward orientation binding.[10]

Equilibrium association constants were determined on the ^{32}P-labeled restriction fragment from pATK4, which contains the inserted sequence shown in figure II.5. The insert contains match and single base pair mismatch sites for both forward and reverse binding orientations. DNase I footprinting results are shown below (Figures II.6–8). Control compound **ATK-iix-77** binds to the forward match site with an affinity of 3.1 x 10^9 M^{-1}. This compound also binds the reverse match site with an affinity of 4.1 x 10^8 M^{-1}, thus favoring forward binding by 7.5-fold.

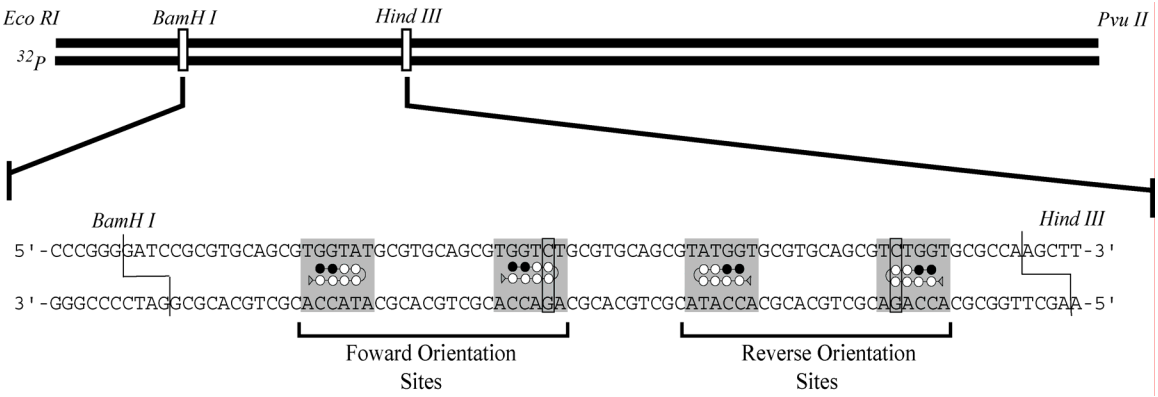

Figure II.5. Diagram of the restriction fragment insert from pATK4 used for DNase I footprinting assays. The insert contains the forward orientation match site (left), a single base pair mismatch for the forward orientation site (center-left), the reverse orientation match site (center-right), and a single base pair mismatch for the reverse orientation site (right).

Compounds possessing the (R) stereochemistry both bind the forward match site with high affinity (5.1 x 10^9 M^{-1} and 6.3 x 10^9 M^{-1}, for **ATK-iix-73** and **ATK-iix-74**, respectively). These polyamides show reduced binding at the reverse match site, with association constants of 1.4 x 10^8 M^{-1} and 5.9 x 10^7 M^{-1}, for **ATK-iix-73** and **ATK-iix-74**, respectively.

The (S)-amine compound **ATK-iix-75** binds to the forward match site with 1.2 x 10^7 M^{-1} affinity and the reverse match site with an association constant < 3 x 10^6 M^{-1}. The (S)-acylated amine compound **ATK-iix-76** does not show binding at either site up to 300 nM concentrations. The DNase I footprinting results are summarized in table II.1.

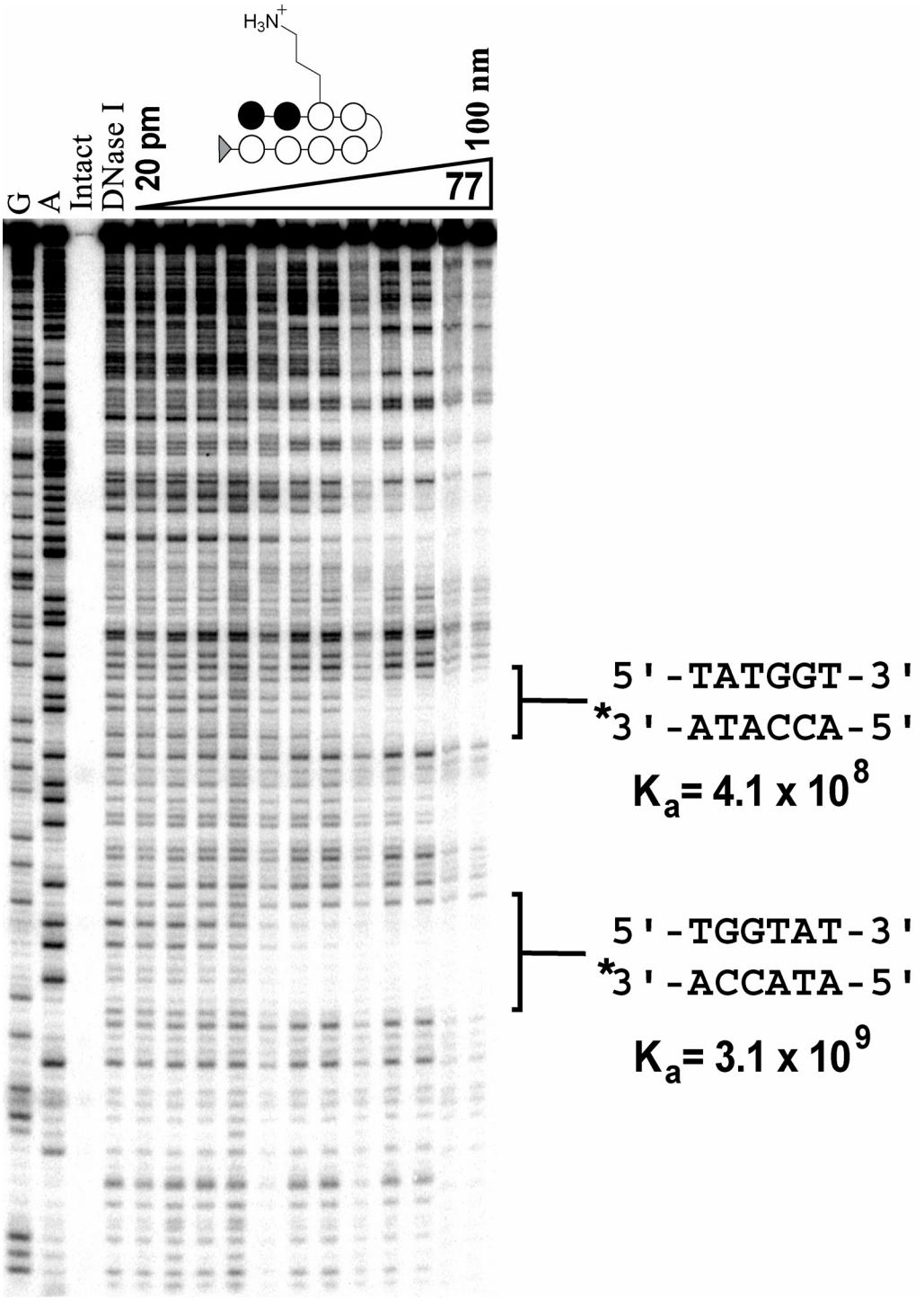

Figure II.6. DNase I footprinting assay on pATK4. Lanes from left to right are G sequencing reaction, A sequencing reaction, intact DNA, lanes 4–15 contain 0, 20pM, 50 pM, 100 pM, 1 nM, 2 nM, 5 nM, 10 nM, 20 nM, 50 nM, 100 nM concentrations of **ATK-iix-77**. Equilibrium association constants shown at right.

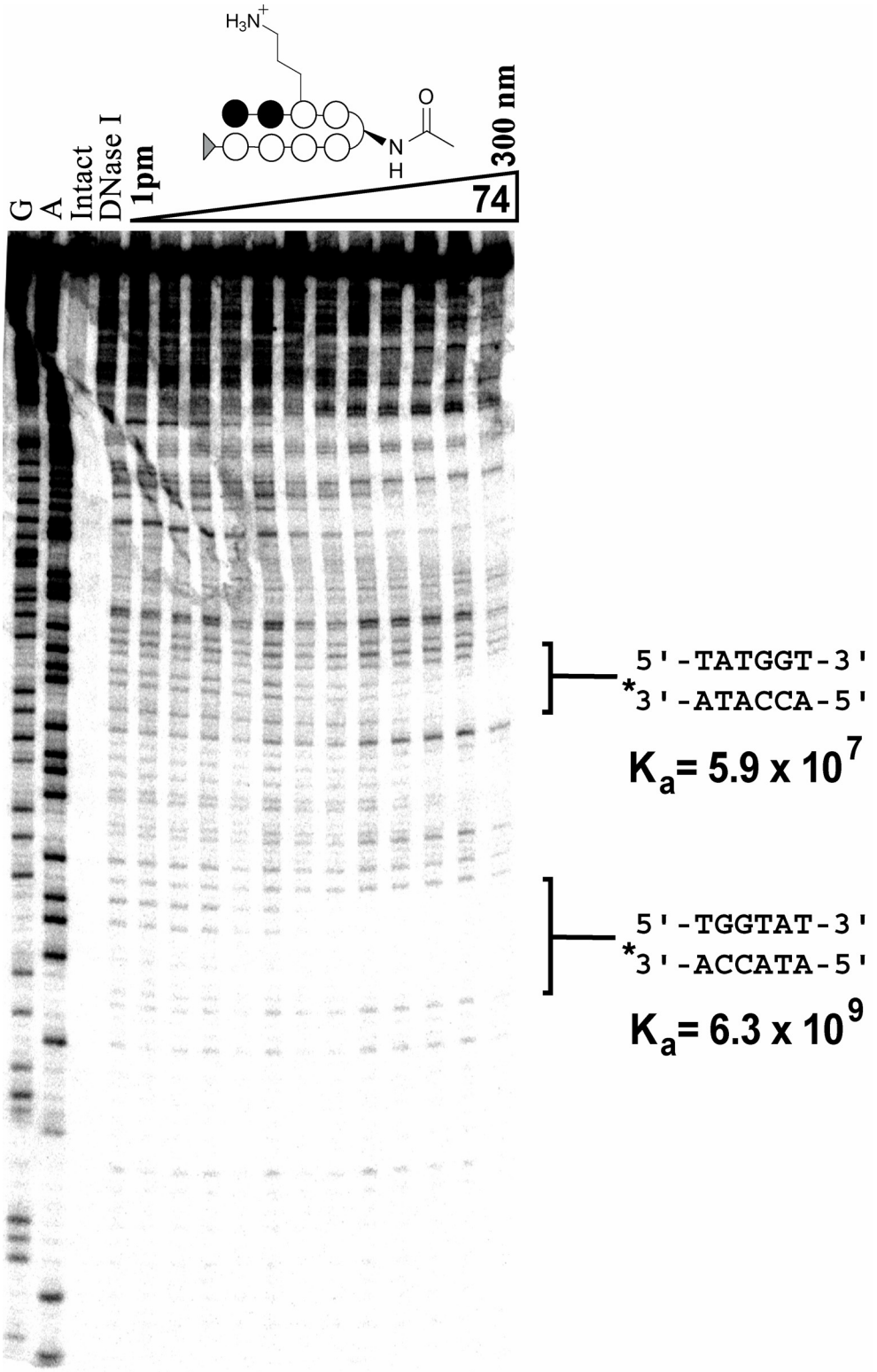

Figure II.7. DNase I footprinting assay on pATK4. Lanes from left to right are G sequencing reaction, A sequencing reaction, intact DNA, lanes 4–16 contain 0, 20pM, 50 pM, 100 pM, 1 nM, 2 nM, 5 nM, 10 nM, 20 nM, 50 nM, 100 nM, 300 nM concentrations of **ATK-iix-74**. Equilibrium association constants shown at right.

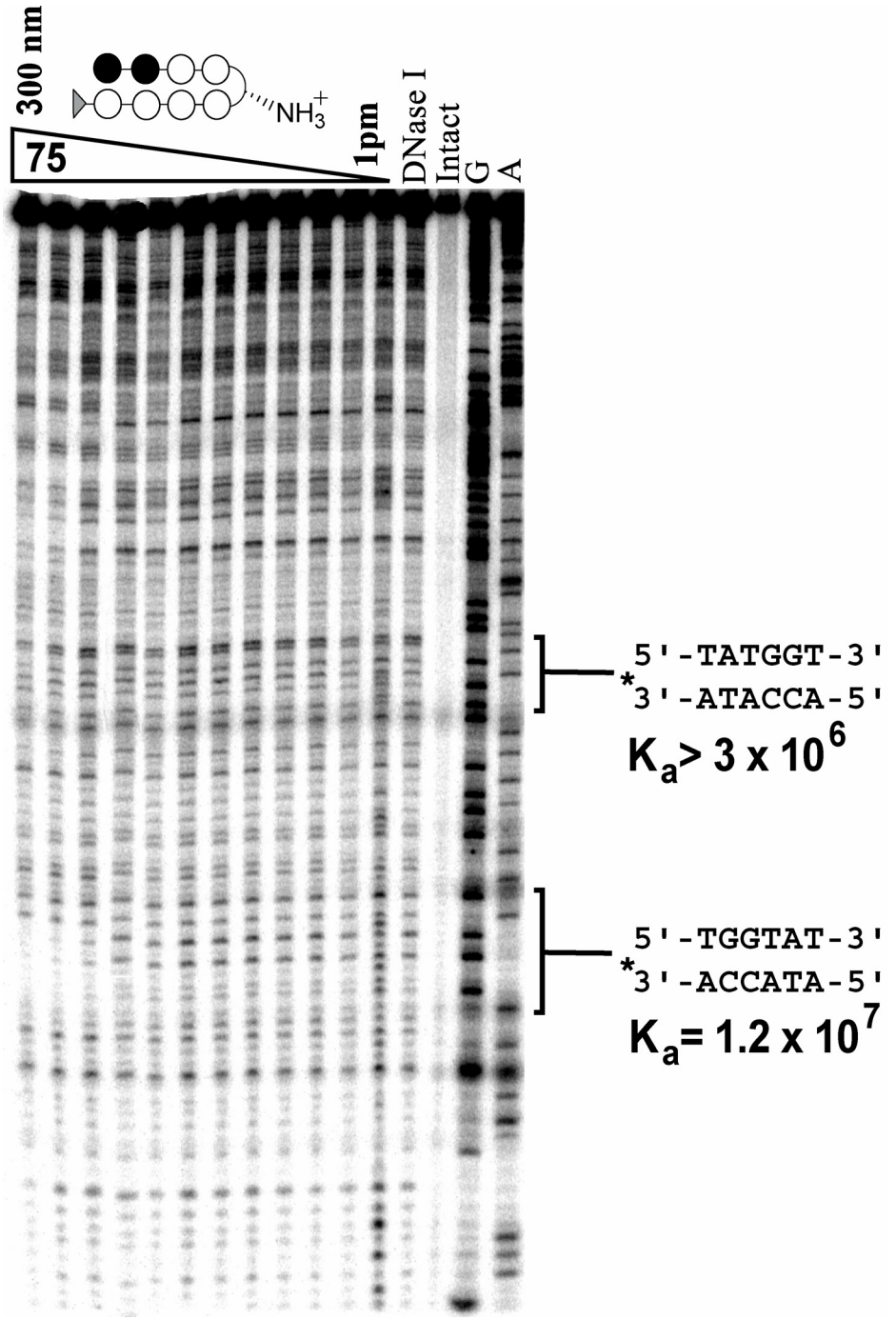

Figure II.8. DNase I footprinting assay on pATK4. Lanes from right to left are A sequencing reaction, G sequencing reaction, intact DNA, lanes 4–16 contain 0, 20pM, 50 pM, 100 pM, 1 nM, 2 nM, 5 nM, 10 nM, 20 nM, 50 nM, 100 nM, 300 nM concentrations of **ATK-iix-75**. Equilibrium association constants shown at right.

Table II.1. Affinity association constants for tailless polyamides.[a]

Polyamide	Forward Match Site 5′-T<u>GGTT</u>A-3′	Reverse Match Site 5′-A<u>TTGG</u>T-3′	Forward Orientation Preference (5'→ 3')[b]
ATK-iix-77	3.1×10^9	4.1×10^8	7.5
ATK-iix-73	5.1×10^9	1.4×10^8	36
ATK-iix-74	6.3×10^9	5.9×10^7	107
ATK-iix-75	1.2×10^7	$< 3 \times 10^6$	>4
ATK-iix-76	$< 3 \times 10^6$	$< 3 \times 10^6$	--

a. Each association constant is the average of three quantitative footprint titrations. Values are reported in units of M^{-1}. Standard deviations are no more than 8% of each reported value. b. Orientation preference calculated as the ratio of the binding affinity at the forward match site versus the reverse match site.

Conclusion.

With the advent of solid-phase synthesis methodologies allowing for the synthesis of hairpin polyamides with truncated C-terminal tails, we were interested in whether these tailless polyamides exhibit any binding orientation preference. Also, we were interested in whether the orientation preference could be controlled or reinforced by the introduction of a chiral amine at the turn position.

Tailless polyamide **ATK-iix-77** shows good binding affinities to both the forward and reverse match sites. This tailless polyamide exhibits only a 7.5-fold preference for the forward site (over the reverse site). This is in stark contrast to the β-Dp analog of this compound, which exhibits a 500-fold orientation preference. Specificities over single base pair mismatches in both orientations were >100-fold.

The (R) stereochemistry at the turn should favor the forward binding orientation. Indeed, when the (R) amine is installed (**ATK-iix-73**), the compound shows increased affinity for the forward match site and reduced affinity at the reverse match site (with

respect to unfunctionalized control **ATK-iix-77**). This results in a 36-fold preference for the forward orientation. When the bulk of the chiral group is increased to the acylated amine (**ATK-iix-75**), the affinity at the reverse binding site is further decreased. This compound exhibits a 106-fold preference for the forward binding site. Thus, the (R) chiral turn acts as a determinant for "forward" orientation preference. Indeed, it is able to restore "forward" orientation preference to tailless polyamides.

Neither of the compounds possessing the (S)-stereochemistry is able to bind any of the sites with reasonable affinities. Indeed, only the (S)-amine compound **ATK-iix-74** showed any binding at all. While this enantiomer was hypothesized to favor the reverse binding orientation, the compound favors the forward site by 4-fold.

We have shown that tailless polyamides exhibit severely decreased orientation preference with respect to the C-terminal β-Dp analogs. Clearly, the tail functionality does account for some of the orientation preference exhibited by hairpin polyamides. Installation of a chiral turn with (R)-stereochemistry is able to restore the orientation preference for the forward binding orientation for tailless hairpin polyamides. Conversely, use of a chiral turn with (S)-stereochemistry is unable to force reverse binding.

Thus, while complete control of binding orientation of tailless polyamides was not achieved, it was found that researchers should be careful to install an (R)-chiral amine or acylated amine on tailless polyamides in order to obtain molecules that are specific for the forward orientation match site over the reverse orientation match site.

Materials and Methods.

Polyamides were synthesized on solid support as previously described.[9] Propylamino pyrrole was installed as previously described.[11]

ATK-iix-73. Synthesized on solid support and cleaved from resin according to literature procedures.[12] UV (H_2O) λ_{max} 310 nm (68720). MALDI-TOF-MS calcd. for $C_{45}H_{60}N_{19}O_8$ (M + H): 1096.1. Found 1096.4.

ATK-iix-74. Synthesized on solid support and cleaved from resin according to literature procedures.[12] UV (H_2O) λ_{max} 310 nm (68720). MALDI-TOF-MS calcd. for $C_{45}H_{60}N_{19}O_8$ (M + H): 1096.1. Found 1096.3.

ATK-iix-75. Synthesized on solid support and cleaved from resin according to literature procedures.[12] UV (H_2O) λ_{max} 310 nm (68720). MALDI-TOF-MS calcd. for $C_{45}H_{60}N_{19}O_8$ (M + H): 1181.2. Found 1181.2.

ATK-iix-76. Synthesized on solid support and cleaved from resin according to literature procedures.[12] UV (H_2O) λ_{max} 310 nm (68720). MALDI-TOF-MS calcd. for $C_{45}H_{60}N_{19}O_8$ (M + H): 1181.2. Found 1181.6.

ATK-iix-77. Synthesized on solid support and cleaved from resin according to literature procedures.[12] UV (H_2O) λ_{max} 310 nm (68720). MALDI-TOF-MS calcd. for $C_{45}H_{60}N_{19}O_8$ (M + H): 1124.2. Found 1124.3.

Construction of plasmid DNA. Plasmid pATK4 was prepared by hybridization of complementary sets of synthetic oligonucleotides. The hybridized insert was individually ligated into *Bam*HI/*Hind*III-linearized pUC19 using T4 DNA ligase. *E. coli* JM109 high efficiency competent cells were then transformed with the ligated plasmid. Plasmid DNA from ampicillin-resistant white colonies was isolated using a Qiagen Wizard MidiPrep kit. The presence of the desired insert was determined by dideoxy sequencing. Concentration of prepared plasmid was determined by UV by the relationship 1 OD_{260} unit = 50 μg/mL duplex DNA.

Preparation of ^{32}P-end-labeled restriction fragments. Plasmid pATK4 was linearized with *Eco*RI and *Pvu*II restriction enzymes. The linearized plasmids were then treated with Klenow enzyme, deoxyadenosine 5'-[α-^{32}P]triphosphate, and thymidine 5'-[α-^{32}P]triphosphate for 3' labeling. The reactions were loaded onto a 7% nondenaturing polyacrylamide gel. The desired band was visualized by autoradiography and isolated. Chemical sequencing reactions were done according to published methods.

Quantitative DNase I footprinting.[13] DNase I footprinting reactions were carried out as previously described. Photostimulable storage phosphorimaging plates (Storage Phosphor Screen from Molecular Dynamics) were pressed flat against gel samples and exposed for 12–16 hours. Imaging of storage phosphor screens was accomplished on a Molecular Dynamics 425E PhosphorImager and the data analyzed using ImageQuant v. 3.2 software.

Binding energetics. Quantitative DNase I footprint titration experiments (10 mM Tris-HCl, 10 mM KCl, 10 mM $MgCl_2$, 5 mM $CaCl_2$, pH 7.0, 22 °C) were performed on the 3'-^{32}P end labeled 270 bp *Eco*RI/*Pvu*II restriction fragment from pATK4. Equilibrium association constants for polyamides **ATK-iix-73 - 77** on the designed binding sites were determined by calculating a fractional saturation value at the site, for each polyamide concentration, and fitting the data to a modified Hill equation.

References.

1. Dervan, P. B.; Edelson, B. S., *Current Opinion in Structural Biology*, **2003,** *13*, 284–299.

2. Rucker, V. C.; Melander, C.; Dervan, P. B., *Helvetica Chimica Acta*, **2003,** *86*, 1839–1851.

3. Hawkins, C. A.; de Clairac, R. P.; Dominey, R. N.; Baird, E. E.; White, S.; Dervan, P. B.; Wemmer, D. E., *Journal of the American Chemical Society*, **2000,** *122*, 5235–5243.

4. Pelton, J. G.; Wemmer, D. E., *Journal of the American Chemical Society*, **1990,** *112*, 1393–1399.

5. Fagan, P.; Wemmer, D. E., *Journal of the American Chemical Society*, **1992,** *114*, 1080–1081.

6. Pelton, J. G.; Wemmer, D. E., *Proceedings of the National Academy of Sciences of the United States of America*, **1989,** *86*, 5723–5727.

7. Fagan, P.; *Ph. D. Thesis*; University of California Berkeley, Berkeley, **1996**.

8. Herman, D. M.; Baird, E. E.; Dervan, P. B., *Journal of the American Chemical Society*, **1998,** *120*, 1382–1391.

9. Belitsky, J. M.; Nguyen, D. H.; Wurtz, N. R.; Dervan, P. B., *Bioorganic & Medicinal Chemistry*, **2002,** *10*, 2767–2774.

10. Swalley, S. E., **1996**, Unpublished Results.

11. Rucker, V. C.; Foister, S.; Melander, C.; Dervan, P. B., *Journal of the American Chemical Society*, **2003,** *125*, 1195–1202.

12. Baird, E. E.; Dervan, P. B., *Journal of the American Chemical Society*, **1996,** *118*, 6141–6146.

13. Trauger, J. W.; Dervan, P. B., Footprinting methods for analysis of pyrrole-imidazole polyamide/DNA complexes. In *Drug-Nucleic Acid Interactions*, 2001; Vol. 340, pp 450–466.